Research Report

2001-41T

Adjustable-Speed Single-Phase IM Drive with Reduced Number of Switches

M. Chomat, T.A. Lipo*

Institute of Electrical Engineering
Czech Academy of Sciences
Dolejskova 5, 182 02 Prague
Czech Republic

*Wisconsin Power Engineering
Research Center
University of Wisconsin - Madison
Madison, WI 53706

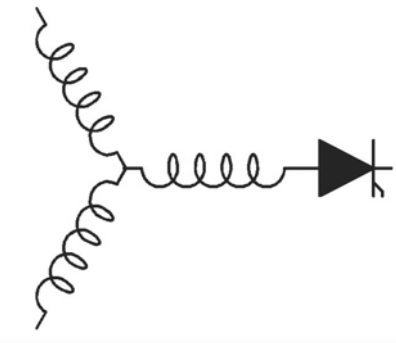

Wisconsin
Electric
Machines &
Power
Electronics
Consortium

University of Wisconsin-Madison
College of Engineering
Wisconsin Power Electronics Research Center
2559D Engineering Hall
1415 Engineering Drive
Madison WI 53706-1691

Adjustable-Speed Single-Phase IM Drive With Reduced Number of Switches

Miroslav Chomat, *Member, IEEE*, and Thomas A. Lipo, *Fellow, IEEE*

***Abstract*—A novel low-cost single-phase induction machine drive containing only two controlled solid-state switches is presented. The drive is intended for heating, ventilation, and air conditioning or a similar type of application requiring variable-speed operation with a fan-type load characteristic. An experimental drive based on the proposed setup has been built to verify its practical viability and to analyze its properties. The paper presents the results obtained from an investigation into this new topology and discusses the properties and characteristics of the drive for the entire speed range from 0 to 60 Hz.**

***Index Terms*—AC motor drives, converters, induction motor drives, single-phase machines.**

I. Introduction

LARGE portions of electrical energy produced in developed countries are consumed for heating, ventilation, and air conditioning (HVAC) in residential areas and for similar applications in the industrial sphere. At present, most of these applications, especially those with lower nominal power, utilize fixed-speed drives and their regulation is achieved primarily by throttling the output flow of the media [1]. Therefore, there is a great potential for energy savings if one manages to introduce energy efficient variable-speed drives into these areas on a massive scale. The problem, however, lies in generally much higher prices for conventional variable-speed drives compared to fixed-speed ones, which is the reason why so much attention has recently been paid to unconventional drive setups with reduced number of solid-state switches [2], [3] or to drives using cheaper to manufacture single-phase machines [4]–[8].

This paper focuses on properties of a drive that uses a single-phase machine of permanent-split capacitor type to drive a fan-type load with variable mechanical speed. To generate the supply voltage with variable frequency a converter with the minimal number of active switches and diodes is used. Such a system cannot fully satisfy requirements of dynamically demanding applications, but could represent a technically and economically feasible solution for HVAC or other similar applications.

Paper IPCSD 03–014, presented at the 2001 Industry Applications Society Annual Meeting, Chicago, IL, September 30–October 5, and approved for publication in the IEEE TRANSACTIONS ON INDUSTRY APPLICATIONS by the Industrial Drives Committee of the IEEE Industry Applications Society. Manuscript submitted for review May 1, 2002 and released for publication February 24, 2003. This work was supported in part by the National Science Foundation under Grant Award 9820434 and by the Grant Agency of the Czech Republic under Grant 102/02/0554.

M. Chomat is with the Institute of Electrical Engineering, Academy of Sciences of the Czech Republic, 182 02 Prague, Czech Republic (e-mail: chomat@iee.cas.cz).

T. A. Lipo is with the Department of Electrical and Computer Engineering, University of Wisconsin, Madison, WI 53706 USA (e-mail: lipo@engr.wisc.edu).

Digital Object Identifier 10.1109/TIA.2003.811778

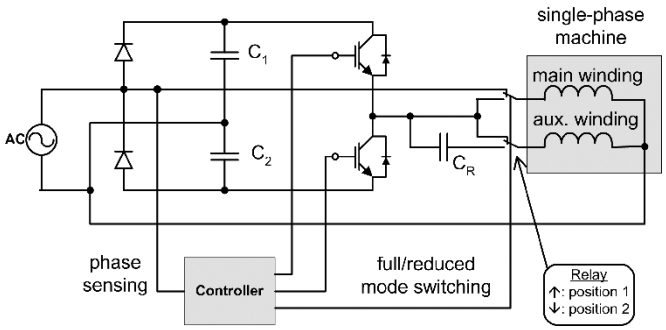

Fig. 1. Scheme of system under investigation.

II. System Description

A simplified scheme of the system under consideration is in Fig. 1. In this system a front-end voltage doubler is connected to a single-phase supply. The output portion of the converter consisting of two insulated gate bipolar transistor (IGBT) or MOSFET switches generates a pulsewidth-modulated (PWM) output supplying one or both stator windings of a single-phase machine. The single-phase machine is considered of the permanent-split capacitor type with the main and auxiliary windings of generally different number of turns. According to the position of the relay contacts at the output of the inverter, one of two principal modes of operation may be selected. These modes are the full-speed mode (position 1) and the reduced-speed mode (position 2).

In the full-speed mode, the main winding is connected directly to the mains and is, therefore, supplied with voltage of the nominal network frequency and amplitude. The inverter produces voltage for the auxiliary winding with the same frequency. The amplitude and the phase of this voltage with respect to the mains are adjusted with the semiconductor switches to achieve a precise 90° phase shift with respect to the main winding and with ampere turns equal to that of the main winding so that optimal operation of the machine can be realized. Hence, operation at rated line frequency nominally exceeds the performance of a normal capacitor run machine operated from a single phase supply since simultaneous 90° phase shift and ampere turn balance can never be exactly achieved with a simple capacitor in the auxiliary winding.

Reduced-speed operation is characterized by the fact that both stator windings are fed from the inverter. The phase shift between the currents in the main and auxiliary windings of the machine is now maintained by means of an ac capacitor

connected in series with the auxiliary winding. The frequency of the supply voltage can be continuously varied from zero to the nominal frequency of the mains and the mechanical speed of the machine varies accordingly. As the run capacitor can only be optimized for a specific supply frequency and machine slip at which the series connection of the run capacitor and the auxiliary winding is in partial resonance, the correct angle between the phase currents cannot be maintained for all the supply frequencies. This may lead to a certain increase in torque pulsations in machine operation at speeds significantly far from the nominal design speed.

The generation of the triggering pulses for the solid-state switches and the state of the output relay are controlled by a single-chip microcontroller. For correct function of the drive in the full-speed mode, it is necessary to synchronize the inverter output with the mains and, therefore, phase sensing of the mains voltage needs to be implemented in the controller.

III. Mathematical Model

A numerical model of the considered system has been developed based on the space phasor description of a single-phase induction machine. The electric machine being considered may be described by the following set of ordinary differential equations in the stator reference coordinate frame under the commonly used simplifying assumptions

$$u_{S\alpha} = R_{S\alpha} i_{S\alpha} + L_{S\alpha} \frac{di_{S\alpha}}{dt} + L_{M\alpha} \frac{di_{R\alpha}}{dt} \tag{1}$$

$$u_{S\beta} = R_{S\beta} i_{S\beta} + L_{S\beta} \frac{di_{S\beta}}{dt} + L_{M\beta} \frac{di_{R\beta}}{dt} \tag{2}$$

$$0 = R_{R\alpha} i_{R\alpha} + L_{R\alpha} \frac{di_{R\alpha}}{dt} + L_{M\alpha} \frac{di_{S\alpha}}{dt} + \frac{1}{a} \omega_m (L_{R\beta} i_{R\beta} + L_{M\beta} i_{S\beta}) \tag{3}$$

$$0 = R_{R\beta} i_{R\beta} + L_{R\beta} \frac{di_{R\beta}}{dt} + L_{M\beta} \frac{di_{S\beta}}{dt} - a\omega_m (L_{R\alpha} i_{R\alpha} + L_{M\alpha} i_{S\alpha}) \tag{4}$$

where

$$a = \frac{N_{S\beta}}{N_{S\alpha}} \tag{5}$$

is the ratio between the effective numbers of turns in the auxiliary and the main stator windings. Subscript α denotes variables in the main winding and subscript β denotes variables in the auxiliary winding. Parameters and quantities with subscripts S and R are those in the stator and in the rotor, respectively. The rotor parameters are referred to the stator. Mechanical speed ω_m is in electrical degrees.

The instantaneous electromagnetic torque produced by the machine is then given by the equation

$$T_e = p\left[a(L_{M\alpha} i_{S\alpha} + L_{R\alpha} i_{R\alpha}) i_{R\beta} - \frac{1}{a}(L_{M\beta} i_{S\beta} + L_{R\beta} i_{R\beta}) i_{R\alpha}\right] \tag{6}$$

where p is the number of pole pairs.

These equations can be directly used to represent the machine in a dynamic Simulink model of the system and can also serve as a starting point for derivation of a phasor model for computing steady-state characteristics. In some cases, a double revolving field theory has also been used in the analysis [9], [10].

TABLE I
Motor Rating and Parameters

Power:	¾ h.p.	R_{1m}	9 Ω
Voltage:	230 V	R_{1a}	22 Ω
Frequency:	60 Hz	R_2	10 Ω
Speed:	1110 rpm	L_{1m}	390 mH
Aux/Main turns ratio:	1.37	L_{1a}	730 mH
Run capacitor:	10 μF	p	6

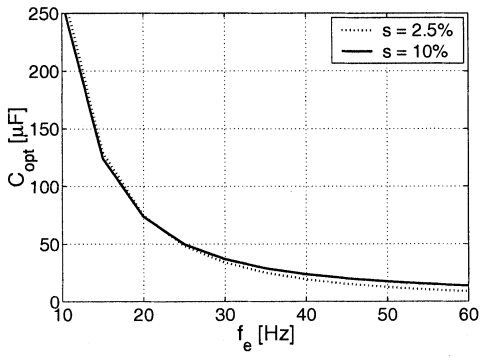

Fig. 2. Optimal run-capacitor capacitance.

IV. Numerical Simulation

The properties of the proposed drive setup were first analyzed by means of numerical simulation. The parameters of a practical 3/4-hp machine from an existing commercial blower were used. The main parameters of the machine are in Table I. A supply voltage of 220 V_{rms} at the input of the drive was considered. A steady-state mathematical model was used to determine the operating points of the machine under various working conditions and to calculate the optimal setting of the drive.

The optimal value of capacitance of the run capacitor to be put in series with the auxiliary winding was calculated for the considered machine from the double revolving field theory. For such capacitance, maximal ratio between forward and backward rotating magnetic fields is achieved in the machine. The resulting values for the supply frequency in the range 10–60 Hz are in Fig. 2. The characteristics for two different values of slip, 2.5% and 10%, are presented. It can be seen that there is only little difference between the values for the two considered slips. This difference would be more significant for higher values of slip. The optimum value of capacitance may not entirely compensate for the torque pulsations in all cases and additional resistances in the main or in the auxiliary winding might be required to achieve precisely symmetrical magnetic field in the machine.

The calculated dependence of the breakdown torque on the supply frequency and on the series capacitance is shown in Fig. 3. The constant voltage-to-frequency ratio was assumed and the slip was considered to have a constant value of 7.5%. The operating point with the maximal breakdown torque may still not be the optimal operating point in practice as the torque pulsations could impair operation of the machine in some areas. The resulting optimal capacitance for normal 60-Hz operation

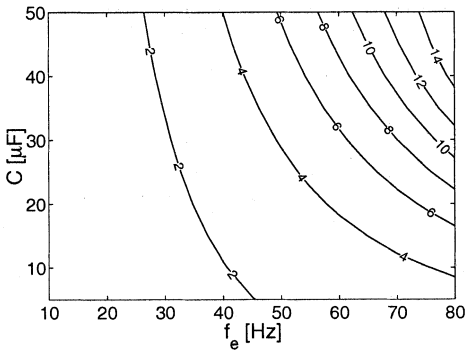

Fig. 3. Breakdown torque dependence for slip $= 7.5\%$.

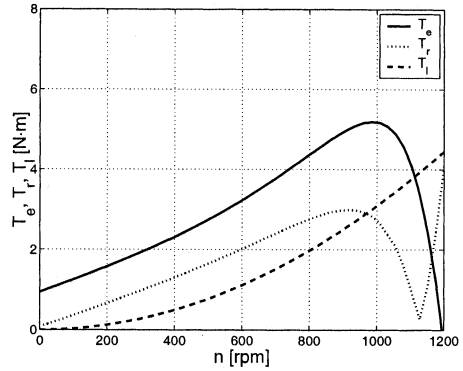

Fig. 4. Torque–speed characteristics, standard operation.

would be 10 μF, which agrees with the value recommended by the manufacturer of the original drive.

A. Full-Speed Operation

First, standard operation of the machine with a run capacitor of 10 μF, which the motor was designed for, was simulated to obtain a reference for the assessment of the quality of the proposed drive setup. The machine was fed with a supply voltage of 220 $V_{\rm rms}$ and 60 Hz. Fig. 4. shows the torque–speed characteristics, where the solid line denoted T_e represents the resulting electromagnetic torque of the machine and the dotted line denoted T_r shows the amplitude of the torque pulsations caused by unbalanced voltage supply of the motor. The dashed line depicts the considered fan load torque–speed characteristic where $T_L \approx n^2$. Fig. 5 then shows the dependences of the current magnitudes in the main, I_m, and the auxiliary, I_a, windings.

Second, full-speed mode operation of the proposed drive was investigated. The corresponding electrical configuration of the system in this case is shown in Fig. 6. The inverter supplying the auxiliary winding was controlled so that it generated a voltage of the same amplitude but shifted by 86° from the phase of the mains to achieve phase quadrature of the currents. The difference from voltage quadrature is given by the fact that the ratios between the real and imaginary parts of the impedances in the main and auxiliary windings are not equal to each other. The optimal phase angle between the voltages across the main and auxiliary windings was analytically determined based on the double revolving field theory from the parameters of the main and auxiliary windings in the considered machine so that the produced torque pulsations were minimized for the nominal speed [11].

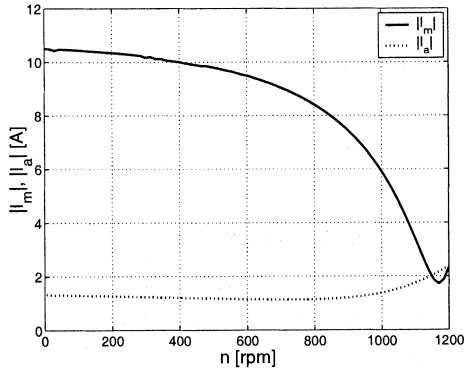

Fig. 5. Stator currents–speed characteristics, standard operation.

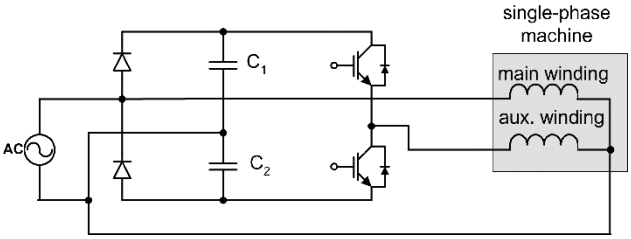

Fig. 6. Scheme of system under investigation, full-speed mode.

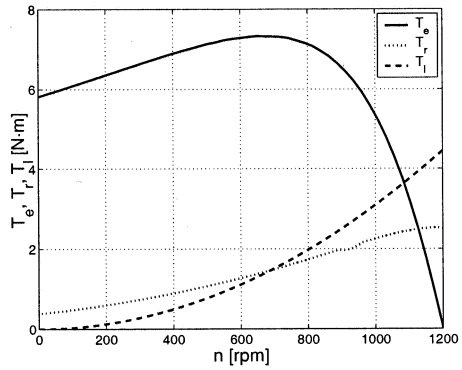

Fig. 7. Torque–speed characteristics, full-speed mode.

Fig. 7 shows the torque–speed characteristics of the drive in the full-speed mode. It can be noted that the machine has quite high starting torque when fed in this manner. The relatively high value of the torque ripple near the nominal speed is mainly due to the limitation of the voltage amplitude generated by the inverter. Ideally balanced operation would require the magnitude of the voltage for the auxiliary winding to be approximately 30% above the magnitude of the voltage supplying the main winding for this particular machine. This is, however, not achievable with the considered front-end part of the converter and the employed PWM method. The dependences of the magnitudes of currents in the main and auxiliary windings on the mechanical speed are presented in Fig. 8. It can be seen that the current in the auxiliary winding is significantly smaller over the range of speed considered here implying a relatively low rating of the inverter needed.

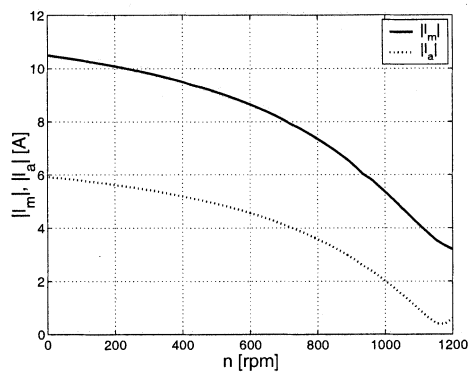

Fig. 8. Stator currents–speed characteristics, full-speed mode.

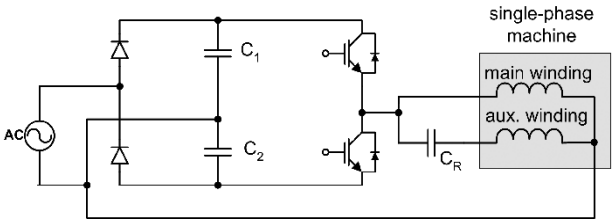

Fig. 9. Scheme of system under investigation, reduced-speed mode.

Comparison of Figs. 7 and 8 with Figs. 4 and 5 reveals that the proposed drive setup provides in the full-speed mode significantly higher starting as well as breakdown torques than the permanent split-capacitor motor. On the other hand, the produced torque ripple is higher for the proposed setup. The stator currents are comparable in both cases for the nominal operating speed.

B. Reduced-Speed Operation

In the reduced-speed mode, the machine is operated in the same manner as a fixed-capacitor machine as can be seen in Fig. 9. That is, the supply frequency is not fixed and may be varied in a certain range. The choice of the optimal value of the capacitance is not as straightforward as in the case of the constant supply frequency. The optimal operation can now be achieved just in one operating point and for the other combinations of frequency and speed the currents will not be in exact quadrature, which gives rise to torque pulsations in other operating points.

The behavior of the machine supplied by voltages of various frequencies and with different capacitor sizes applied in series with the auxiliary winding were investigated [12]. The magnitude of the supply voltage was adjusted in direct proportion to the supply frequency. From the obtained results, a capacitor of 20 μF appears to be a suitable compromise for the speed range from 0 to 60 Hz considered here for this application and such a capacitor is, therefore, considered in the following.

The torque–speed characteristics are shown in Fig. 10 together with the assumed load torque characteristic. The load is a fan type with a square dependence of torque on speed. It may be noted that the machine can drive the load at all chosen supply frequencies. Fig. 11 shows what torque pulsations develop in this case. The amplitude of these pulsations is plotted against the mechanical speed for different supply frequencies and can

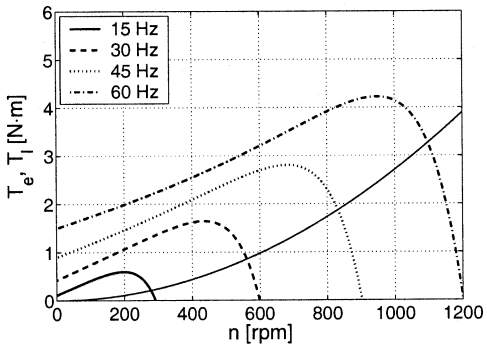

Fig. 10. Torque–speed characteristics, $C_R = 20\ \mu$F.

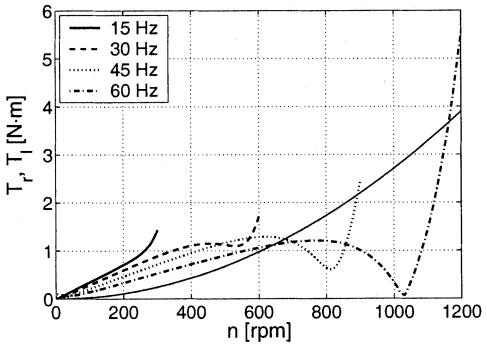

Fig. 11. Torque-ripple amplitudes, $C_R = 20\ \mu$F.

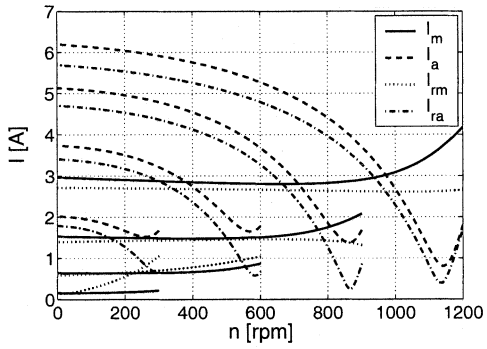

Fig. 12. Stator and rotor currents, $C_R = 20\ \mu$F.

be compared again with the corresponding load torque characteristic. The minimum of these pulsations for particular supply frequencies takes place near the operating point of the machine. The machine now operates with virtually zero pulsations for a supply frequency of 60 Hz and a speed of 1050 r/min. The amplitudes of the stator and rotor currents in the machine are shown in Fig. 12. The corresponding supply frequencies applied in the figures may be identified from the maximum mechanical speeds achieved. A significant difference between the currents in the main and the auxiliary windings should be noticed.

In actual variable-speed operation, the mechanical speed of the machine adjusts itself so that a balance between the electromagnetic torque and the load torque is achieved for a given supply frequency. Fig. 13 shows the electromagnetic torque and the amplitude of torque pulsations as functions of mechanical speed. The torque pulsations have a salient local minimum at a mechanical speed of about 900 r/min. The slip is nearly constant

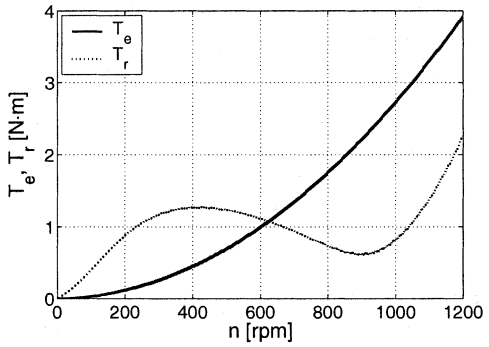

Fig. 13. Electromagnetic torque and torque-ripple amplitude, $C_R = 20\ \mu F$.

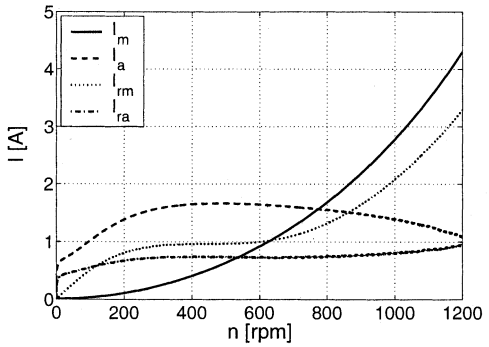

Fig. 14. Stator and rotor currents, $C_R = 20\ \mu F$.

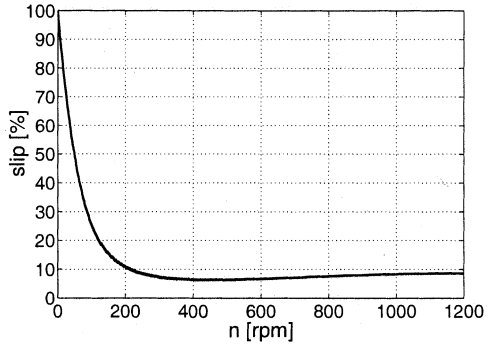

Fig. 15. Slip of machine, $C_R = 20\ \mu F$.

above 300 r/min and lies between 7%–10%. Corresponding current amplitudes are in Fig. 14. The slip varied with speed according to the graph in Fig. 15.

The developed numerical model of the drive was employed in simulation of dynamic behavior of the system in different transient processes. Figs. 16 and 17 present the results of simulation of a speed control sequence. The supply frequency was linearly increased from 0 to 30 Hz for 0.5 s first, for another 0.5 s it was kept constant, and then it was increased at the same rate until 57 Hz (95% of 60 Hz) was achieved. At that moment, the full-speed mode took over and speed was maintained for another 0.5 s. The same sequence, but in a reverse order, was applied to decrease the speed until the machine stalled. The run capacitor of 30 μF was used in this simulation.

The electromagnetic torque and mechanical speed are given in Fig. 16 and the stator currents in the main and auxiliary windings in Fig. 17. The electromagnetic torque pulsations in Fig. 16

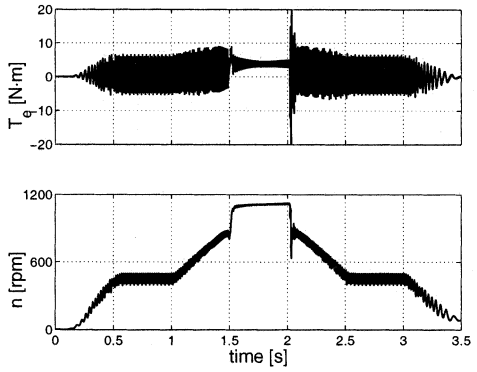

Fig. 16. Torque and speed during control of drive.

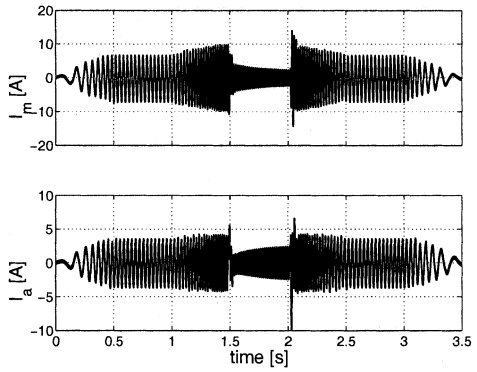

Fig. 17. Stator currents during control of drive.

are smoothed out by the moment of inertia of the rotor and the driven load to a large extent and, in general, should not cause significant problems in a common HVAC application. The instantaneous changeover from the full-speed mode to the reduced-speed mode and vice versa introduced brief intervals of current and torque transients. It is possible to reduce these transients by more sophisticated timing as is shown in the following.

V. Experimental Results

An experimental drive has been developed in order to verify the theoretical results and the practical viability of the proposed setup. The control algorithm was implemented in a control board based on a digital signal processor TMS320C240. The algorithm generated a PWM voltage waveform with variable amplitude and frequency with the possibility to synchronize the output with the line voltage. A set of measurements has been carried out in order to verify the theoretical results and analyze the behavior of the practical drive. Operation both at full speed (60 Hz) and at reduced speeds has been tested for various load torques.

The results for the full-speed operation are presented first. To take the different numbers of turns in the main and auxiliary windings into account, the currents in the auxiliary winding are multiplied by the proper turns ratio and correspond, therefore, rather to current layers in the machine. The plotted trajectory directly indicates then the quality of the supply voltage for the motor. Fig. 18 shows the shape of the stator current layer for the full-speed operation when the phase shift between the voltages fed to the main and auxiliary windings is 90°. The motor

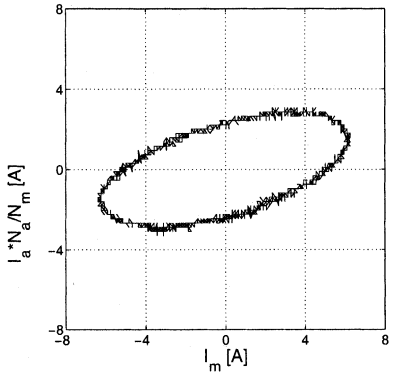

Fig. 18. Measured stator current layer, f $= 60$ Hz, $\varphi = 0°$.

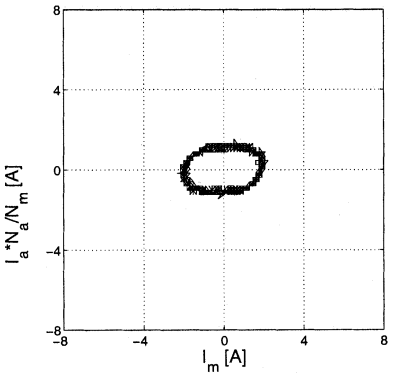

Fig. 19. Measured stator current layer, f $= 30$ Hz, $C_R = 30\ \mu$F.

connected to a dynamometer and loaded by 270 W rotated at 923 r/min. The current layer forms an ellipse with an angular deviation of the main axis from the real axis of the reference frame. It means that the angle between the currents in the main and auxiliary windings is different from the optimal 90°, which is caused by different impedances of the main and auxiliary windings.

Operation of the drive at half speed is illustrated in Figs. 19 and 20. A readily available ac capacitor of 30 μF was used as a motor-run capacitor this time. The mechanical speed was 527 r/min and the load was 65 W. Fig. 20 shows the supply voltages at the stator windings terminals. It should be noted that the voltage stress for the auxiliary windings increases significantly in this mode of operation. This is due to the fact that the PWM voltage from the converter summed with the voltage drop caused by the fundamental-harmonic component of the stator current across the run capacitor appears at the machine terminals.

In general, sudden switching between reduced-speed and full-speed modes may cause a transient response notable both in torque or speed and in stator currents of the machine. There are several methods available to keep these effects within some predetermined limits. Probably the ideal way would be to use exact timing of switching which would minimize the transients and consume the minimal time. This is, however, not practical in the case of a considered low-cost and low-power drive. In our case, intermediate time intervals have simply been inserted during which the current transients are allowed to die out before applying the supply voltage of different frequency. This is shown in Figs. 21 and 22. The current in the main winding is

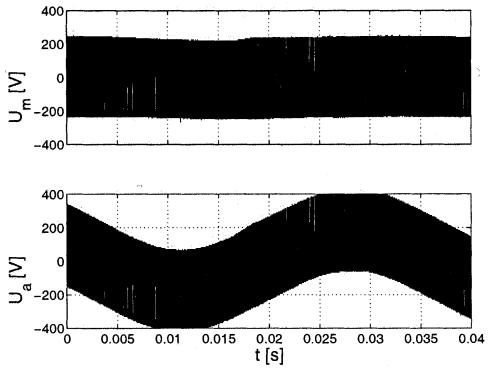

Fig. 20. Stator voltages, f $= 30$ Hz, $C_R = 30\ \mu$F.

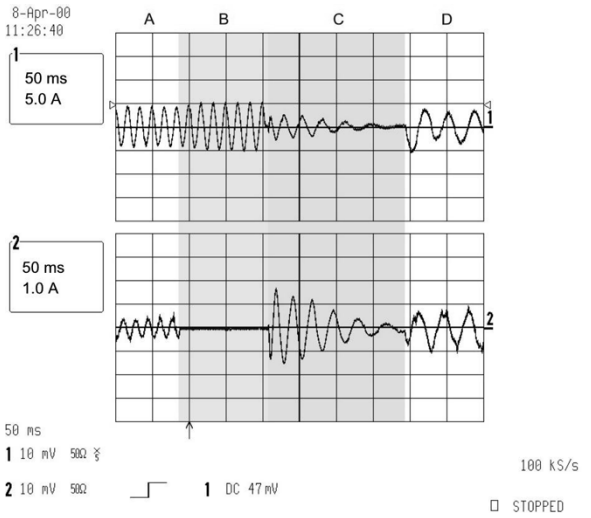

Fig. 21. Measured stator currents during transition from full- to reduced-speed operation.

in trace 1 and the current in the auxiliary winding in trace 2. Fig. 21 illustrates the transition from the full-speed in interval *A* to reduced-speed operation in interval *D*. Within interval *B* only the main winding is connected to the mains while the inverter is idle and the currents may flow only through the flywheel diodes of the inverter. In interval *C* both windings are disconnected and the current transient in auxiliary winding excited by disconnecting the main winding has enough time to decay. A similar approach, but in reverse order, is applied for the transition from half-speed to full-speed operation in Fig. 22. The entire transition process is synchronized with the phase of the supply voltage. In case the drive is connected to a load with relatively high moment of inertia, precautions need to be taken in order to maintain the dc-link voltage within some safety limits during braking.

VI. Conclusion

The results presented in the paper suggest that the proposed drive setup could be an economically and technically viable alternative to fixed-speed and conventional variable-speed drives in many HVAC applications and the like having a load torque which varies with the square of speed. The operation of the drive is not optimal throughout the entire speed range and significant torque ripple may arise in some operating points, but this should

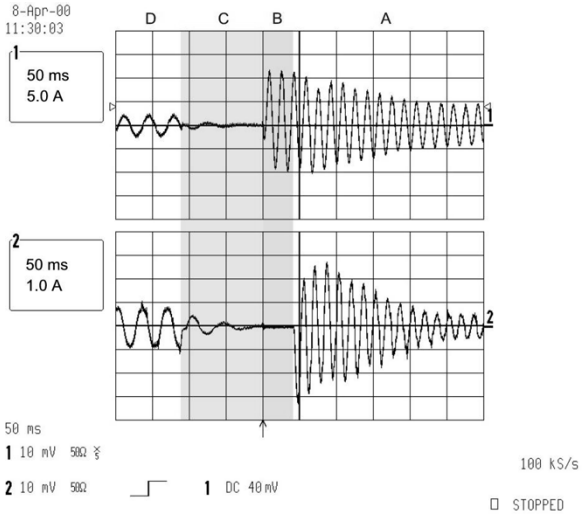

Fig. 22. Measured stator currents during transition from reduced- to full-speed operation.

not disqualify it for most low- or even medium-power applications. A great advantage of the proposed drive is its robustness and low manufacturing cost. Increased energy efficiency should ensure a relatively quick payback of the additional investment in comparison to a fixed-speed drive. Moreover, the possibility of adjusting the mechanical speed in a broad range would provide customers with a higher level of users comfort. The prototype of the proposed drive was built and tested in a laboratory and the theoretical results obtained were proven experimentally.

REFERENCES

[1] H. N. Hickok, "Adjustable speed—a tool for saving energy losses in pumps, fans, blowers, and compressors," *IEEE Trans. Ind. Applicat.*, vol. 21, pp. 124–136, Jan./Feb. 1985.

[2] B. A. Welchko and T. A. Lipo, "A novel variable frequency three-phase induction motor drive system using only three controlled switches," in *Conf. Rec. IEEE-IAS Annu. Meeting*, 2000, pp. 1468–1473.

[3] J. Klima, "Analytical model of induction motor fed from four-switch space vector PWM inverter. Time domain analysis," *Acta Tech. CSAV*, vol. 44, pp. 393–410, 1999.

[4] D. G. Holmes and A. Kotsopoulos, "Variable speed control of single and two phase induction motors using a three phase voltage source inverter," in *Conf. Rec. IEEE-IAS Annu. Meeting*, 1993, pp. 613–620.

[5] L. Julian, R. S. Wallace, and P. K. Sood, "Multi-speed control of single-phase induction motors for blower applications," *IEEE Trans. Power Electron.*, vol. 10, pp. 72–77, Jan. 1995.

[6] N. P. van der Duijn Schouten, B. M. Gordon, R. A. McMahon, and M. S. Boger, "Integrated drives as single-phase motor replacement," in *Conf. Rec. IEEE-IAS Annu. Meeting*, 1999, pp. 922–928.

[7] M. B. R. Correa, C. B. Jacobina, A. M. N. Lima, and E. R. C. da Silva, "Single-phase induction motor drives systems," in *Proc. IEEE APEC'99*, vol. 1, 1999, pp. 403–409.

[8] E. R. Benedict and T. A. Lipo, "Improved PWM modulation for a permanent-split capacitor motor," in *Conf. Rec. IEEE-IAS Annu. Meeting*, 2000, pp. 2004–2010.

[9] P. C. Krause, O. Wasynczuk, and S. D. Sudhoff, *Analysis of Electric Machinery*. New York: IEEE Press, 1995.

[10] E. R. Collins, "Torque and slip behavior of single-phase induction motors driven from variable-frequency supplies," *IEEE Trans. Ind. Applicat.*, vol. 28, pp. 710–715, May/June 1992.

[11] M. Chomat and T. A. Lipo, "Adjustable-speed drive with single-phase induction machine for HVAC applications," in *Proc. IEEE PESC'01*, 2001, pp. 1446–1451.

[12] ——, "Adjustable-speed single-phase IM drive with reduced number of switches," in *Conf. Rec. IEEE-IAS Annu. Meeting*, 2001, pp. 1800–1806.

Miroslav Chomat (M'94) received the M.S. degree in electrical power engineering from the Czech Technical University, Prague, Czechoslovakia, in 1988, and the Ph.D. degree in electrical engineering from the Institute of Electrical Engineering, Academy of Sciences of the Czech Republic (ASCR), Prague, Czech Republic, in 1994.

He is currently with the Institute of Electrical Engineering, ASCR. From 1999 to 2000, he was a Honorary Research Fellow at the University of Wisconsin, Madison. His research interests include analysis, modeling, and control of electrical machines, drives, and power units.

Thomas A. Lipo (M'64–SM'71–F'87) is a native of Milwaukee, WI. He received the B.E.E. and M.S.E.E. degrees from Marquette University, Milwaukee, WI, in 1962 and 1964, respectively, and the Ph.D. degree in electrical engineering from the University of Wisconsin, Madison, in 1968.

From 1969 to 1979, he was an Electrical Engineer in the Power Electronics Laboratory of Corporate Research and Development, General Electric Company, Schenectady, NY. He became a Professor of Electrical Engineering at Purdue University, West Lafayette, IN, in 1979 and, in 1981, he joined the University of Wisconsin, Madison, in the same capacity. He is presently the W.W. Grainger Professor for Power Electronics and Electrical Machines.

Dr. Lipo has received the Outstanding Achievement Award from the IEEE Industry Applications Society, the William E. Newell Field Award from the IEEE Power Electronics Society, and the 1995 Nicola Tesla IEEE Field Award from the IEEE Power Engineering Society for his work. In November 2002, he was elected a Fellow of the Royal Academy of Engineering. Over the past 30 years, he has served the IEEE in numerous capacities, including President of the IEEE Industry Applications Society.